

# Integrated Slanted Microneedle-LED Array for Optogenetics

Ki Yong Kwon, *Student Member*, Anton Khomenko, Mahmoodul Haq, and Wen Li, *Member, IEEE*

**Abstract**— This paper presents a three-dimensional (3-D) flexible micro light emitting diode ( $\mu$ -LED) array for selective optical stimulation of cortical neurons. The array integrated individually addressable  $\mu$ -LED chips with slanted polymer-based microneedle waveguides to allow precise light delivery to multiple cortical layers simultaneously. A droplet backside exposure method was developed to monolithically fabricate slanted microneedles on a single polymer platform. A wafer-level assembly technique was demonstrated, which permits large-scale, high-density system integration. The electrical, optical, thermal, and mechanical properties of the 3-D slanted microneedle-LED array were characterized experimentally.

## I. INTRODUCTION

Electrical neural stimulation has been a powerful tool for decades in electrophysiology and clinical neuroscience, to treat neurological problems including sensory deficits, Parkinson's disease, epilepsy, and depression [1]. However, its limitations such as unpredictable current pathways, electrical artifacts, and non-selectivity of the target neurons increase the demands for a new technology. Recent developments in optogenetics can target specific types of neurons with sub-millisecond temporal precision, by direct optical stimulation of genetically modified neurons in the brain tissue [2], [3].

For *in vitro* and head-fixed *in vivo* applications, various optical stimulation systems have been reported such as a laser or light emitting diodes (LEDs)-coupled optical fiber [4], micro LED arrays [5], band-filtered white light [4], and a focused laser beam through a microscope [6]. However, for a research requiring freely behaving subjects, only a few light delivery methods are available, such as a laser-coupled optical fiber and a head-mountable single LED system [7]. Spatial resolution of these systems is poor and the tethered optical fiber restricts natural behavior of the subjects.

We recently reported an epidural optical stimulating approach using an Opto- $\mu$ ECoG array that contained a transparent micro electrocorticogram ( $\mu$ ECoG) electrode array with integrated  $\mu$ -LEDs [8]. We demonstrated for the first time that a 32 individually addressable  $\mu$ -LED array could evoke neural activities not only on the surficial cortical layer but also in deep cortical layers (with a depth of 600  $\mu$ m). Although this 32  $\mu$ -LED array significantly improved the spatial resolution of the optical stimulation, its

\*Research supported by National Science Foundation and Michigan State University.

K. Kwon and W. Li are with the Electrical and Computer Engineering Department, Michigan State University, East Lansing, MI 48824 USA (phone: +1-517-353-7832, e-mail: [kwonki3@egr.msu.edu](mailto:kwonki3@egr.msu.edu), [wenli@egr.msu.edu](mailto:wenli@egr.msu.edu)).

A. Khomenko and M. Haq are with the Mechanical Engineering Department, Michigan State University, East Lansing, MI 48824 USA.

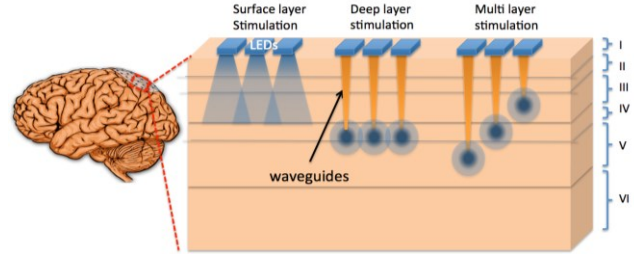


Figure 1. Comparison of different optical stimulation methods using cortical LED array

depth resolution had a severe limitation. In addition, the depth control of the epidural optical stimulation required relatively high input voltage in order to deliver light to the deep cortical layers. Finally, selective stimulation of a target layer is impossible with the surface light source. To overcome these challenges, we have developed a 3-D multi-LED array that integrated  $\mu$ -LED chips with microneedle waveguides to minimize the scattering of LED lights in the brain tissue and achieve high spatial resolution [9].

In this study, we further improve the spatial resolution of the 3-D multi-LED array in depth by proposing a slanted waveguide array. Fig.1 showed a comparison of the newly proposed slanted array with the two previously reported methods. Integration of individually addressable  $\mu$ -LED chips with varying-length microneedles allows precise light delivery to the target neurons in individual cortical layers.

## II. DESIGN

As shown in Fig. 2 (a), our proposed array contains 32 embedded  $\mu$ -LED light sources on a polyimide substrate. The physical dimension of the array was  $2 \times 2$  mm<sup>2</sup> with 16 ( $4 \times 4$  grid) channels per each hemisphere to meet the specifications of bilateral visual cortices in rats. Integrated LED light sources allow for the implementation of a truly untethered system, which is crucial for chronic implant in freely behaving animals.

The slanted microneedle array can be fabricated separately on a PDMS substrate and bonded with the multi-LED array using shape-matching assembly. Several approaches for making slanted microneedle structures have been reported, but they either required a specialized machine and material [10], or lacked a control of the microneedle size that determines light coupling efficiency [11]. In this paper, a new technique, “droplet backside exposure” (DBE), is introduced, which utilizes the height variance in the profile of a droplet to create the slanted microneedle array.

The DBE method uses surface energy differences between two adjacent contact areas of a PDMS substrate to define the curvature of a droplet. As shown in Fig. 2 (b),

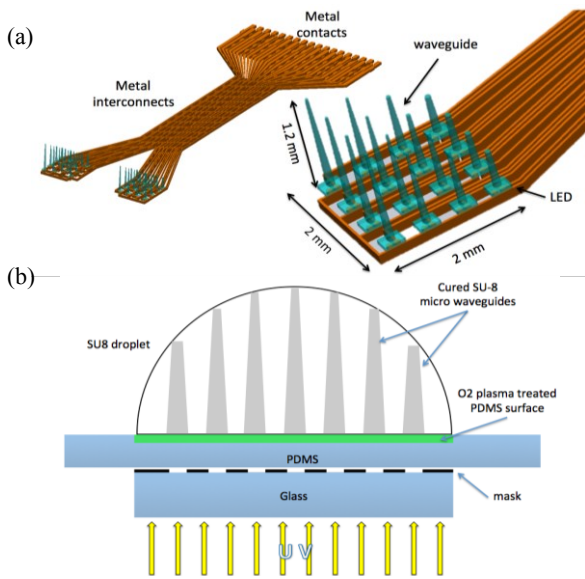


Figure 2. (a) Conceptual diagram of the proposed 3-D slanted array. (b) Principle of the SU-8 droplet backside exposure method

a dome-shaped SU-8 droplet with a designed base size can be formed on a patterned hydrophilic area ( $O_2$  plasma treated-PDMS surface) with hydrophobic surroundings (intact PDMS surface). In a certain volume range, the droplet is confined within the boundary between the hydrophilic and hydrophobic regions, due to the difference of the surface energies, and this allows the various height of the droplet by controlling the volume of SU-8. Then the slanted microneedle structures can be formed in the dome structure using a backside exposure [11]. Details of the DBE method are reported in [12]. This technique allows us to control lengths, tip and bottom diameters of individual microneedles without sophisticated equipment and complex microfabrication. Moreover, it is relatively simple with only slight changes from regular lithography processes and permits wafer-level microfabrication for large scale, high-density system integration.

Several objectives are considered to optimize the design of the optical stimulation array. First, the microneedle waveguide must be able to deliver light to the desired cortical layers. In this study, the microneedles with lengths ranging from 400 to 1000  $\mu\text{m}$  were designed to provide an access to multiple cortical layers (layer III to V) in the primary visual cortex (V1) of the rat.

Second, the waveguide must be capable of evoking neural activity at the target cortical region. Typically irradiance of 1-5  $\text{mW}/\text{mm}^2$  is required to activate ChR2 expressing neurons [2]. The irradiance and the total flux delivered at the target region can be controlled by the tip size of the microneedle and the size of the tip was selected from the simulation results.

Third, the microneedle should be mechanically durable to penetrate the brain tissue without breaking, while minimizing damages to the brain tissue. In this study, we used a needle-shaped configuration, which had a wide base of 200  $\mu\text{m}$  and tapers to a sharp tip of 50  $\mu\text{m}$ .

Finally, the light sources must be individually addressable and distributed over the targeting cortical area.

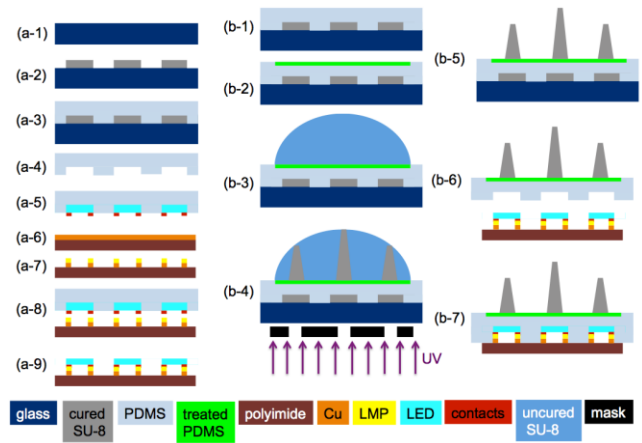


Figure 3. Fabrication process

Surface mounted  $\mu\text{-LED}$  chips ( $220 \times 270 \times 50 \mu\text{m}^3$ , wavelength peak at 460 nm, Cree® TR2227TM) coupled with the waveguide allow a precise optical stimulation in a single or multiple spots simultaneously.

### III. FABRICATION

In order to reduce fabrication complexity, the multi-LED array and the slanted microneedle array were fabricated and calibrated separately. Then the system was assembled by polymer bonding of individual components with SU-8. Detailed fabrication was divided into two steps and described in the following sections (Fig. 3).

#### A. Multi-LED array assembly

(a-1) A 3" silicon wafer was cleaned. (a-2)  $\sim 30 \mu\text{m}$  SU-8 layer was spun onto the wafer and patterned as the mold for fabricating a PDMS stamp. (a-3) PDMS was poured over the SU-8 mold to form the stamp, which contained cavities matching the shape of the LED chip. (a-4) After curing for 40 min at 95  $^\circ\text{C}$ , the PDMS stamp was peeled off from the mold. (a-5) 32 LED dies were aligned in the cavities of the stamp with metal pads facing outward. A substrate for LED assembly was fabricated using Pyralux®AP (AP7163E, DuPont). (a-6) 3" Pyralux® wafer was cut and cleaned, followed by Cu wet-etching. (a-7) Low melting point (LMP) solder (melting point at  $\sim 62 \text{ }^\circ\text{C}$ , 144 ALLOY Field's Metal, Rotometals, Inc) was applied on the contacts. (a-8) The PDMS stamp with the embedded LEDs was aligned to match the metal contacts of the LEDs with the pre-soldered receiver sites on the substrate. (a-9) The substrate with the aligned PDMS stamp was heated on a hot plate at 90  $^\circ\text{C}$  for 30 sec. The PDMS stamp was peeled off carefully after the substrate was cooled down to 40  $^\circ\text{C}$ . The substrate, with the attached LEDs, was then submerged into a hot acidic water bath (90  $^\circ\text{C}$ , pH of 2.0) for 1 min. This process permits the fine adjustment of LED alignment and the formation of electrical connection in a self-assembly manner [13].

#### B. Slanted microneedle array fabrication and assembly

(b-1) A 3" glass wafer was cleaned and went through a dehydration bake. a  $\sim 50 \mu\text{m}$  SU-8 layer was spun onto the wafer and patterned as the mock LEDs. A thin layer of

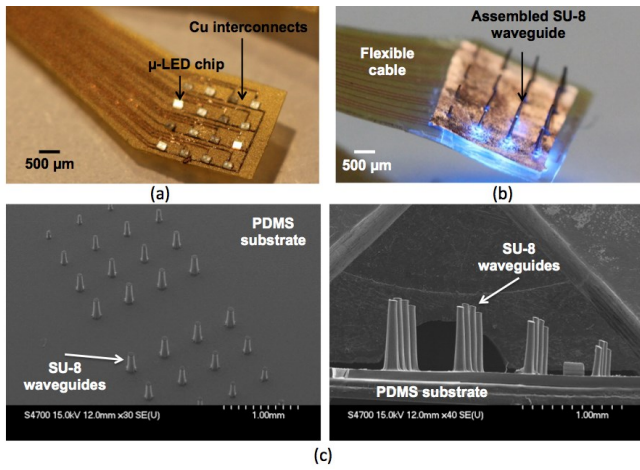


Figure 4. Images of a representative LED array (a) before and (b) after assembly with a slanted microneedle array. (c) SEM images of slanted arrays

PDMS was spun on the SU-8 master to make cavities that matched the shape of the LED. (b-2) After the PDMS was cured for 40 min at 95 °C, photoresist (PR) was patterned on the PDMS substrate to expose 7 mm-diameter circles, followed by oxygen plasma treatment to convert the exposed hydrophobic areas to hydrophilic ones. (b-3) After removal of the PR mask, ~45  $\mu$ L SU-8 (SU-8 3005) was dispensed on top of the plasma treated PDMS surface using a micropipette and (b-4) patterned with the backside exposure to form the microneedles. (b-5) After SU-8 development, the array was polished by O<sub>2</sub> plasma etching and (b-6) the membrane was released from the glass wafer. (b-7) Finally, the microneedle array with the matched LED cavities was aligned onto the corresponding LED chips and bonded with polymer adhesive.

#### IV. EXPERIMENTAL RESULTS

Array prototypes and the SEM images of the slanted  $\mu$ -waveguides were shown in Fig. 4. The optical, electrical, thermal, and mechanical properties of the slanted waveguide array were investigated in this section.

##### A. Optical properties

In this study, we characterized the effect of the geometry of the microneedle on the irradiance and total flux of transmitted blue light, using a ray tracing method (TracePro®, Lambda Research Co., MA, USA). In the simulation, the average irradiance and the total flux were measured at 100  $\mu$ m distance from the microneedle tip, as a function of the tip size. With a small tip size, optical throughputs tended to spread out, resulting in divergent irradiance, while a large tip size led to concentrated irradiance with a confined output beam. The coupling efficiency of the proposed slanted waveguide array was also studied. In this case, we assumed a typical LED radiation angle of ~60° and inserted a 80  $\mu$ m-thick PDMS layer (with a refractive index of 1.46 at 470 nm) between the LED and the SU-8 waveguide (with a refractive index of 1.59 at 470 nm). The estimated coupling efficiency of the waveguide was ~9%, which is closed to the typical coupling efficiency

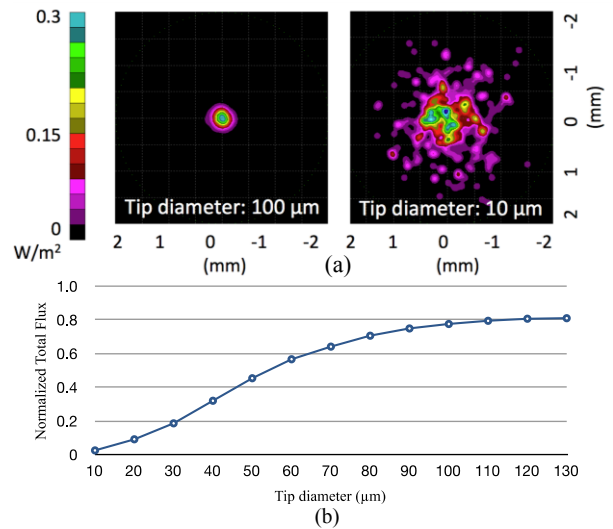


Figure 5. Simulation results: (a) irradiance measurements at a 100  $\mu$ m distance from two tips with diameters of 10  $\mu$ m and 100  $\mu$ m, and (b) normalized total flux measured at a 100  $\mu$ m distance from waveguide tips with different tip diameters (10 – 130  $\mu$ m).

of the butt coupling method [14]. Based on the simulation results, careful selection of the tip size of the microneedle is important in order to deliver sufficient optical throughput to the target area, while permitting easy penetration of the tissue.

To characterize light scattering property of the array, we studied the optical throughput at the tip of the  $\mu$ -waveguide in a scattering media (20% w/w of gelatin). The slanted 3-D multi-LED array was placed on the gelatin media and images of the optical throughput at the tip of the  $\mu$ -waveguide were captured. The activated LEDs was driven by 2.7 V resulting in a power consumption of 3.4 mW, a temperature increase of 0.1 °C, and the light source irradiance of 1 mW/mm<sup>2</sup>. Blue light spectra (wavelength range of 450 – 495 nm) were extracted from the captured image, and the normalized relative light intensity (the maximum intensity as 1) was shown in Fig. 6 (b). A clear ellipsoidal scattering boundary (~600  $\mu$ m in length and ~100  $\mu$ m in width) of the optical throughput, shown in Fig.6 (c).

##### B. Electrical properties

A minimal irradiance of 1 mW/mm<sup>2</sup> must be delivered to the target area to induce action potentials. For surface stimulation, an input voltage of ~2.7 V was used to drive a single  $\mu$ -LED chip to achieve the required optical power output, resulting in a power consumption of 3.4 mW. Considering 9% of the estimated coupling efficiency of the array, the  $\mu$ -LED chip was driven by an input voltage of ~2.9 V to achieve an optical power intensity of 10 mW/mm<sup>2</sup>, resulting in a total power consumption of 17 mW and a temperature increase of ~0.4 °C. Further improvement can be envisioned by narrowing the radiation angle of the LED and optimizing the design of the microneedle.

##### C. Thermal properties

The temperature variation of the LED array was investigated using a high definition infrared camera (Delta Therm HS1570 and the software (DT v.2.19)) with different

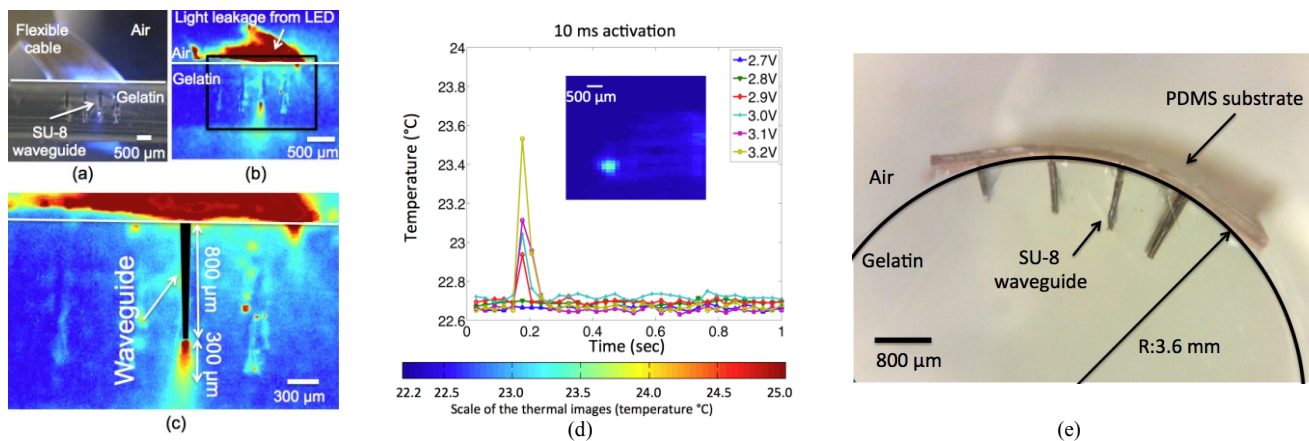


Figure 6. (a) Experimental setting to study optical throughput at the tip of waveguide, (b) relative intensity of the blue light (450-495 nm) extracted from the captured image. (d) Thermal properties: Heat dynamics of the Opto- $\mu$ ECoG array at various input voltages (2.7 V-3.2 V) for 10 ms. (e) Penetration profile of the microneedle array in a curved gelatin substrate.

input voltages (2.7-3.2 V) and activation durations (10, 50, and 100ms, respectively). As expected, both the input voltage and duration of stimulation dramatically changed the temperature profile of the LED. With the low input voltage of 2.7 V, the heat produced by the LED resulted in the local temperature increase of less than 1 °C. The heat dissipated within 50 ms and the LED temperature returned to the baseline point ( $\sim 22.7$  °C). As the input voltage and the activation duration increased, significant heat was generated by the LED, resulting in higher local temperature, larger heat conduction, and longer heat dissipation time. The maximum temperature increase was over 9 °C when the LED was driven by 3.2 V with the 100 ms activation duration.

#### D. Mechanical properties

Finally, we examined the mechanical properties of the array by implanting the array in gelatin (20% w/w) substrates with different curvatures. As shown in Fig. 6 (e), the flexible PDMS substrate wrapped around the curved surface, while the waveguides penetrated perpendicular to the surface. This result demonstrated that a combination of the flexible substrate and the rigid waveguide structure offers potential applications for not only cortical implant but also spinal cord and peripheral nerves implants. Specifically for peripheral nerve implant, each row of waveguides can target different depth of axon bundles in peripheral nerve systems without deformation of the nerves.

#### V. CONCLUSION

The design objectives, fabrication process, and properties of a slanted 3-D multi-LED array for optogenetics were described in this study. The slanted microneedle array was designed to target the layer III - V in V1 of the rat, and a new DBE technique for making slanted microneedle structures was introduced. The simulation results suggested that the irradiation and the total flux of the optical throughput of the microneedle waveguide highly depended on the tip size of the waveguide. The electrical power consumption to achieve the irradiance of 1 mW/mm<sup>2</sup> at the waveguide tip was estimated based on the coupling efficiency of  $\sim 9\%$ . The mechanical properties of the array were studied with the penetration test in the gelatin media and the result

demonstrated possible applications of spinal cord and peripheral nerve implant.

#### REFERENCES

- [1] H. S. Mayberg, A. M. Lozano, V. Voon, H. E. McNeely, D. Seminowicz, C. Hamani, J. M. Schwab, and S. H. Kennedy, "Deep Brain Stimulation for Treatment-Resistant Depression," *Neuron*, vol. 45, no. 5, pp. 651–660, Mar. 2005.
- [2] F. Zhang, A. Aravanis, A. Adamantidis, L. de Lecea, and K. Deisseroth, "Circuit-breakers: optical technologies for probing neural signals and systems," *Nature Reviews Neuroscience*, vol. 8, no. 8, pp. 577–581, 2007.
- [3] O. Yizhar, L. E. Fenno, T. J. Davidson, M. Mogri, and K. Deisseroth, "Optogenetics in neural systems," *Neuron*, vol. 71, no. 1, pp. 9–34, 2011.
- [4] F. Zhang, L. Wang, M. Brauner, and J. Liewald, "Multimodal fast optical interrogation of neural circuitry," *Nature*, vol. 446, pp. 633–639, 2007.
- [5] B. McGovern and E. al, "A New Individually Addressable Micro-LED Array for Photogenetic Neural Stimulation," *Biomedical Circuits and Systems, IEEE Transactions on*, vol. 4, pp. 469–476, 2010.
- [6] R. Hira, N. Honkura, J. Noguchi, and E. al, "Transcranial optogenetic stimulation for functional mapping of the motor cortex," *Journal of Neuroscience*, 2009.
- [7] Y. Iwai, S. Honda, H. Ozeki, and E. al, "A simple head-mountable LED device for chronic stimulation of optogenetic molecules in freely moving mice," *Neuroscience research*, 2011.
- [8] K. Kwon and W. Li, "Opto-ECoG Array: Transparent ECoG Electrode Array and Integrated LEDs for Optogenetics," *Biomedical Circuits and Systems, IEEE Transactions on*, Nov. 2012.
- [9] K. Kwon and W. Li, "Integrated multi-LED array with three-dimensional polymer waveguide for optogenetics," *Micro Electro Mechanical Systems, IEEE 26th International Conference on*, Jan. 2013.
- [10] T. Abaya, M. Diwekar, S. Blair, P. Tathireddy, L. Rieth, G. A. Clark, and F. Solzbacher, "Characterization of a 3D optrode array for infrared neural stimulation," *Biomedical Optics Express*, vol. 3, no. 9, pp. 2200–2219, 2012.
- [11] H. Huang and E. al, "Different fabrication methods of out-of-plane polymer hollow needle arrays and their variations," *J. Micromech. Microeng.*, vol. 17, no. 2, pp. 393–402, Jan. 2007.
- [12] K. Kwon, B. Xiaopeng, and W. Li, "Droplet backside exposure for making slanted SU-8 microneedles," *Medicine and Biology Society, IEEE 35th Annual International Conference on*, Jun. 2013, Submitted for publication.
- [13] H. Onoe, A. Nakai, E. Iwase, K. Matsumoto, and I. Shimoyama, "Temperature-controlled transfer and self-wiring for multi-color light-emitting diode arrays," *J. Micromech. Microeng.*, vol. 19, no. 7, p. 075015, Jun. 2009.
- [14] G. Keiser, *Optical Fiber Commn.* McGraw-Hill Education, 2008.